

Design and Study of a DC/DC Converter for High Power, 14.4 V and 300 A for Automotive Applications

Júlio Cesar Lopes de Oliveira, Carlos Henrique Gonçalves Treviso

Abstract—The shortage of the automotive market in relation to options for sources of high power car audio systems, led to development of this work. Thus, we developed a source with stabilized voltage with 4320 W effective power. Designed to the voltage of 14.4 V and a choice of two currents: 30 A load option in battery banks and 300 A at full load. This source can also be considered as a source of general use dedicated commercial with a simple control circuit in analog form based on discrete components. The assembly of power circuit uses a methodology for higher power than the initially stipulated.

Keywords—DC-DC power converters, converters, power conversion, pulse width modulation converters.

I. INTRODUCTION

THE proposed project is to obtain a high power Switched-Mode Power Supply (SMPS) with high efficiency and low Electromagnetic Interference (EMI), targeted to the automotive sound market. It can also be used to power electronic devices because of the characteristic of stabilized output voltage and even to charge a bank of batteries, because the control is set to obtain two bands of constant output current. A desired feature is the implementation of the project of power and simple control, with discrete components easy to purchase in the domestic market.

The design of the control circuit aims to complete integration of the system with an inrush control, thermal protection triggering fan of heatsink from 35 °C and off the SMPS after 60 °C with stopping operation of the source, frequency synchronization possibility with another control system, generation of eight isolated pulses for driving the switches, feedback loop to control current and voltage outputs and indicative LEDs of operating conditions of the SMPS.

The converter is divided into modules as shown in Fig. 1 and allowing the use of several power stages and automatic dual voltage system with a reduced size resulting in maximum power of 4320 W and high efficiency (above 85%).

The SMPS can be used on power car audio systems, voltage of 14.4 V (usual voltage for charging automotive battery or

Julio C. L. de Oliveira is with the Department of Electrical Engineering, State University of Londrina, Londrina, Pr, Brazil (e-mail: julio@projetric.com.br).

Carlos H. G. Treviso is with the Department of Electrical Engineering, State University of Londrina, Londrina, Pr, Brazil (e-mail: treviso@uel.br).

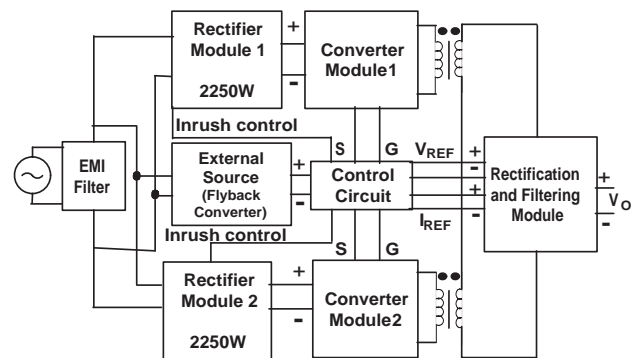


Fig. 1 Complete block diagram of the converter

power supply of sound systems) with full load current of 300 A or as a current source of 30 A to charge batteries [1].

II. THE INPUT RECTIFIER

The AC input protection is accomplished through a thermal-electric breaker 63 A.

We use an input rectifier of the SMPS as shown in Fig. 2, in option of 220 V, we have D_1 , D_2 , D_3 and D_4 acting as a single phase full bridge rectifier with C_1 and C_2 as output filter. With voltage of 127 V we have in the positive half cycle, D_1 and D_4 is on charging C_1 and in the negative half cycle, D_2 and D_3 is on charging C_2 , acting as a voltage doubler because the voltages of C_1 and C_2 adds up. [2]–[9].

The inrush current control was done with three sets of relay and a resistor R as Fig. 2. The relays (normally-open) is closed by a pulse of 12V from the control circuit. Uses three sets of transistors configured as a switch, to actuate the respective relays in parallel, due to high current. To help in the current division between relays were added to an alloy of constantan series with each relay. Three resistors are used in parallel 33 Ω x 5 W, after the control command, the relays are activated send total power to the converter as Fig. 2 [3].

EMI filter (Fig. 1) as show in Fig. 3 with: $C_b = C_f = 470\text{nF}$, $R_f = 15 \Omega$ x 2 W with the inductor L_f 2 x 8 espiras in core NT35/22/22. [10], [11].

Input rectifier has automatic selection for 127 V and 220 V (V_i) shown in Fig.4. These relays will switch to full bridge

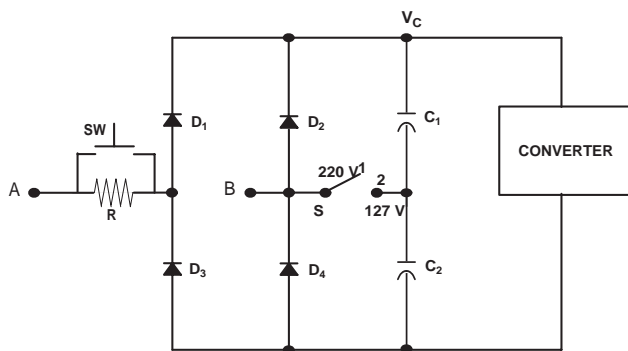


Fig. 2 The Input Rectifier

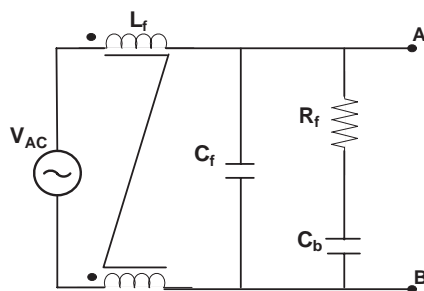


Fig. 3 EMI filter

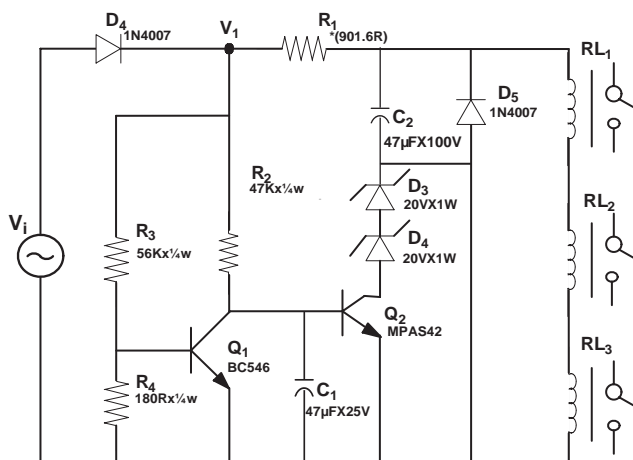


Fig. 4 Selector of input voltage

rectifier (220 V) or doubler (127 V) according to Fig. 2. Transistors Q_1 and Q_2 work as switch entering as off or on according to the input voltage as shown in Table I, triggering the set of the relays RL_1 , RL_2 e RL_3 (dividing the current through the contacts of the relays) [12].

Relay contacts are connected in the position shown by the switch of the input rectifier as shown in Fig. 2.

TABLE I
SUMMARY OF THE STATUS OF COMPONENTS

Components	127V	220V
Q_1	Off	On
Q_2	On	Off
RL_1 , RL_2 and RL_3	On	Off

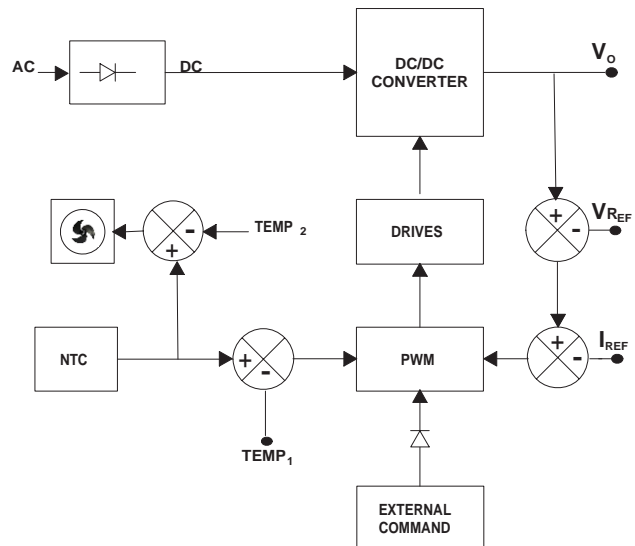


Fig. 5 Block diagram of the control circuit

III. THE CONTROL CIRCUIT

Control block diagram of the Switched-Mode Power Supply (SMPS) is shown in Fig. 5.

Control system is based on the IC 3525 (Regulating Pulse Width Modulators), and operates in closed loop from a reference voltage (V_{ref}) delivering 14.4 V (V_o) and can work as a current source from an adjustable reference current (I_{ref}) allowing two levels of current by switch (30 A or 300 A in full load). The choice of IC 3525 was because its characteristics: internal soft-start, pulse-by-pulse shutdown, adjustable deadtime control and oscillator Sync terminal. [13].

Waveform of output control as show in Fig. 6.

To the source control circuit was used a flyback converter with universal input ($80-240V_{AC}$) and stable output in $12V_{DC}$. The thermal control is performed from NTC thermistor, set to trigger forced ventilation system from 35°C ($TEMP_1$) and off the pulses of control circuit from 60°C ($TEMP_2$ - shutdown) as shown in Fig. 5.

The system has an emergency stop command where the control pulses can be turned off at any time (EXTERNAL COMMAND) as shown in Fig. 5.

Command relays of inrush current control was performed by charging a capacitor, whose time constant RC provides the

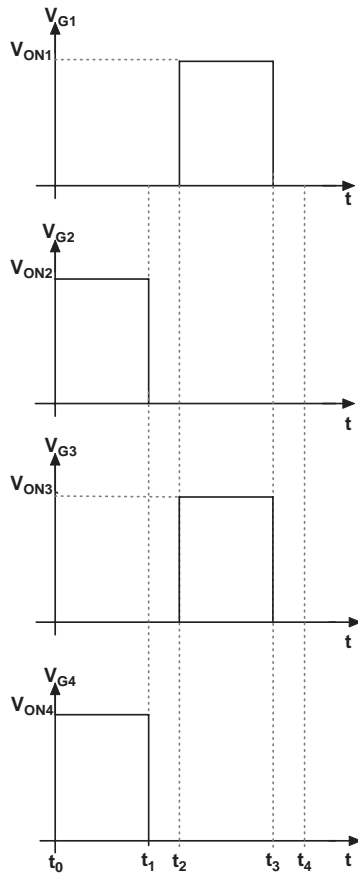


Fig. 6 Waveform of output control circuit

necessary time for charging the capacitors of the input rectifier (C_1 and C_2), before actuate the relays as shown in Fig. 2.

It also has eight drives isolated to enable the use of any type converter producing isolated pulses with voltage above 10V on the triggering of MOSFETs and negative voltage of -3.9V on off, this isolation is provided by the using the pulse transformer drive circuit. [3]

The Control circuit has 47 mm height and 115 mm in length with SMD components as shown in Fig. 7.

Justification of the use of an analog control circuit was simplicity (not requiring any programming) and the ease of acquisition in the market of electronic components.

IV. THE POWER CIRCUIT

The converter full-bridge was chosen to be suitable for power above 1000 W with current doubler because it works with smaller inductors facilitating its construction as shown in Fig. 8 [14]–[16].

Four states are used to analyze the full-bridge with current doubler converter, where each MOSFET as a switch controlled by the control circuit as show in Fig. 6 [17], [18]:

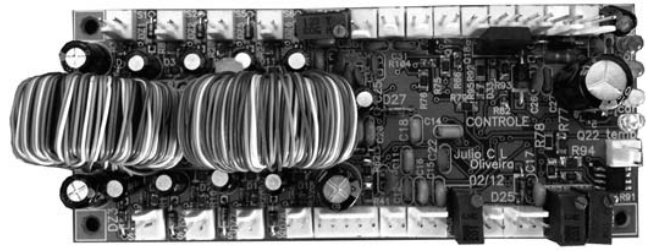


Fig. 7 Control Circuit

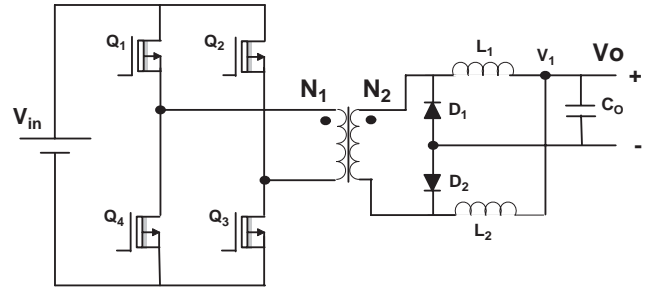


Fig. 8 Full-bridge with current doubler converter

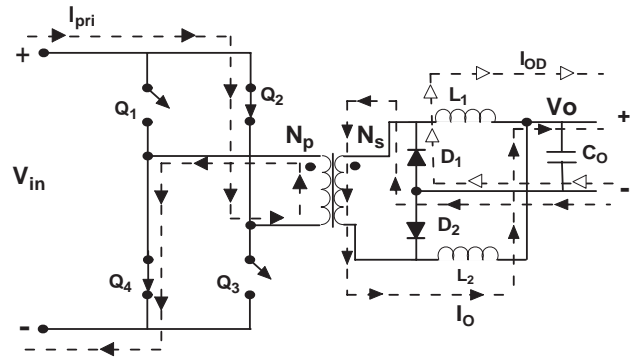


Fig. 9 State 1 of converter

State 1: ($0 < t < t_1$) The switches Q_2 and Q_4 are on and the switches Q_1 and Q_3 are off as shown in Fig. 9, the current I_{pri} is the transformer's primary that induces another electric opposing current on transformer's secondary (I_o) crossing D_1 , L_2 (magnetizing) and load. In this interval, the inductor L_1 demagnetizes through D_1 and loads.

State 2: ($t_1 < t < t_2$) There is a dead time where all the switches are turned off and there was no current in primary and secondary of the transformer. The demagnetization of the inductors L_1 and L_2 allows the passage of the primary current that induces a secondary current on transformer. The demagnetization of the inductors L_1 and L_2 to allow movement of the load current I_o through the diodes D_1 and D_2 as shown in Fig. 10.

State 3: ($t_2 < t < t_3$) The switches Q_1 and Q_3 are

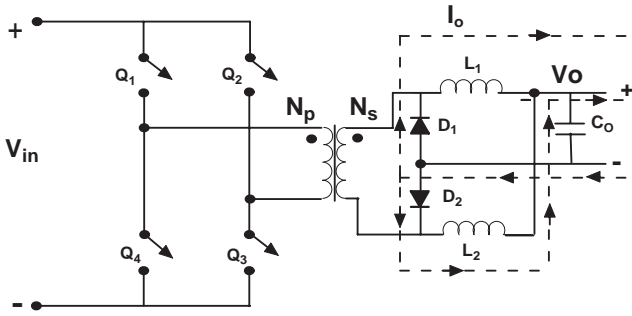


Fig. 10 State 2 of converter

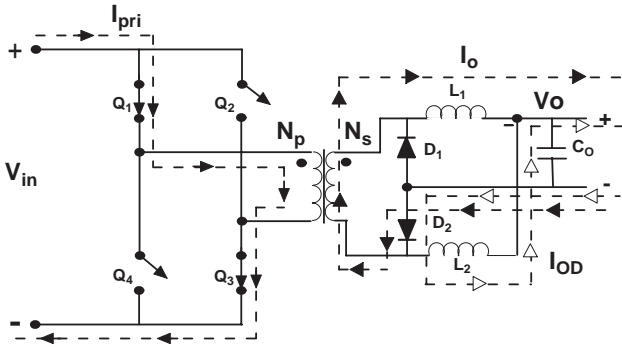


Fig. 11 State 3 of converter

turned off as shown in Fig. 11 allowing the passage of current I_{pri} at the primary of the transformer, this will induce a current in the opposite direction from the secondary of the transformer allowing the passage of current I_o through D_2 , L_1 (magnetizing) and the load. In this interval, the inductor L_2 demagnetizes through D_2 and loads.

State 4: ($t_3 < t < t_4$) There is a dead time again and the circuit behaves as state 2.

Due to the limitation of the power of the switches, it was made a division of the power involved and used two independent modules called CONVERTER MODULE coupled with two transformers with the primary in parallel mode and the secondary in serial mode, to provide the voltage to the rectification module and filtering, as Fig. 1.

On the converter module, aiming the low cost, flexibility and ease of acquiring components, we used four IRF840 MOSFETs connected in parallel with the respective snubber for each MOSFET (Q_1 , Q_2 , Q_3 and Q_4) as Fig. 8.

The filter inductor (L_1 and L_2) according to Fig. 8 divides the total current output (I_o). The value of core energy (E), inductance of each inductor (L), minimal D.C. output current I_{omin} , minimal duty cycle (D_{min}), current density (J) and copper area (A_{cu}) is calculated respectively in (1), (3), (2), (4), (5) and (6) [19], [20].

$$A_p = \left(\frac{2E \times 10^4}{K_u \times K_j \times B_{max}} \right)^{\frac{1}{1-x}} \quad (1)$$

$$E = \frac{1}{2} L \left(\frac{I_o}{2} + I_{omin} \right)^2 \quad (2)$$

$$L = \frac{D_{min} (1 - D_{min}) V_{i \max}}{4N I_{omin} f_s} \quad (3)$$

$$D_{min} = \frac{D_{max}}{V_{i \max}} V_{i \min} \quad (4)$$

$$J = K_j A_p^{-x} \quad (5)$$

$$A_{cu} = \frac{\sqrt{\left(\frac{I_o}{2}\right)^2 + I_{omin}^2}}{J} \quad (6)$$

Where:

- A_p - Product of the window area by the air gap area of the core.
- E - Core energy.
- K_u - Utilization factor of core window.
- K_j - Coefficient current density in the wires.
- B_{max} - Maximum magnetic flux density.
- x - Constant dependent on type of the core of the inductor.
- L - Inductance of each inductor.
- I_o - Maximum D.C. output current.
- I_{omin} - Minimal D.C. output current.
- D_{max} - Maximum duty cycle.
- D_{min} - Minimum duty cycle.
- $V_{i \max}$ - Maximum input voltage.
- $V_{i \min}$ - Minimum input voltage.
- N - Transformation ratio.
- f_s - Switching frequency.
- J - Current density.

The filter capacitors were obtained by taking the variation of rated voltage on the capacitor with respect to satisfaction in the transitory regime (7), and permanent (8), which composes the output filter ripple voltage in (9) [20].

$$\Delta V_{ct} = \frac{2D_{min} (1 - 2D_{min}) V_{i \max}}{8LCN (2f_s)^2} + \frac{L \Delta I_o^2}{CV_o} \quad (7)$$

$$\Delta V_{cp} = 2I_{omin} R_{se} + \Delta I_o R_{se} \quad (8)$$

$$\Delta V_c \geq \Delta V_{ct} + \Delta V_{cp} \quad (9)$$

Where:

- ΔV_{ct} - Capacitor ripple voltage in transitory regime.
- ΔV_{cp} - Capacitor ripple voltage in permanent regime.
- ΔV_c - Total Capacitor ripple.
- C - Capacitance of the filter capacitor.
- ΔI_o - Output ripple current.
- V_o - Output voltage.

- R_{se} - Equivalent series resistance of capacitor.

The value of magnetic flux density (B), number of turns of the transformer primary (N_1), new transformation ratio (N'), secondary current ($I_{sec_{RMS}}$) and secondary copper area ($A_{cu_{sec}}$) is calculated respectively (10), (11), (12), (13) and (14) [12], [19]–[22].

$$B = \frac{V_{i \min}}{V_{i \max}} 2B_{\max} \quad (10)$$

$$N_1 \geq \frac{V_{i \min} D_{\max}}{A_e B f_s} \quad (11)$$

$$N' = 2N = \frac{4D_{\max} (V_{i \min} - 2V_{SD})}{V_o + 2D_{\max} V_F} \quad (12)$$

$$I_{sec_{RMS}} = I_o \sqrt{2D_{\max}} \quad (13)$$

$$A_{cu_{sec}} = \frac{I_{sec_{RMS}}}{J} \quad (14)$$

Where:

- B - Flux density.
- N_1 - Number of turns of the transformer primary.
- A_e - Gap area of the core.
- N' - Transformation ratio for two transformers in parallel.
- V_{SD} - Drain-source voltage of MOSFET.
- V_F - Instantaneous Forward Voltage.
- $I_{sec_{RMS}}$ - Secondary current of transformer (RMS).
- $A_{cu_{sec}}$ - Secondary copper area of the core.

V. DESIGN OF POWER CIRCUIT

The system parameters of the design circuit are:

- For the core EE-65/33/26 $A_p = 30.31 \text{ cm}^2$
- $K_u = 0.4$
- For EE core $K_j = 346.98$
- For IP6 core $B_{\max} = 0.35 \text{ T}$
- For EE core $x = 0.12$
- $I_o = 300 \text{ A}$
- $V_{i \max} = 380 \text{ V}$
- $V_{i \min} = 225 \text{ V}$
- $N = 13.242$
- $f_s = 50 \text{ kHz}$
- $V_o = 14.4 \text{ V}$
- Design rule $\Delta V_c = 5\% V_o = 0.72 \text{ V}$
- $D_{\max} = 0.45$

A. INDUCTOR

The maximum power of the EE-65/33/26 core is obtained in (15).

$$A_p = \left(\frac{2E \times 10^4}{K_u \times K_j \times B_{\max}} \right)^{\frac{1}{1-x}} \quad (15)$$

$$E = 46 \text{ mJ}$$

Using (3) and (15):

$$E = \frac{1}{2} L \left(\frac{I_o}{2} + I_{o \min} \right)^2$$

$$L = \frac{9.18 \times 10^{-2}}{(150 + I_{o \min})^2} \quad (16)$$

Using (4):

$$D_{\min} = \frac{D_{\max}}{V_{i \max}} V_{i \min} = \frac{0.45}{380} 225 = 0.266 \quad (17)$$

Using (3):

$$L = \frac{D_{\min} (1 - D_{\min}) V_{i \max}}{4N I_{o \min} f_s} = \frac{74.19}{2648400 I_{o \min}} \quad (18)$$

Equal to (21) to (18), and obtains the results (19) and (20), which excludes the value greater than I_o (20):

$$I_{o \min 1} = 7.58 \text{ A} \quad (19)$$

$$I_{o \min 2} = 2966.45 \text{ A} \quad (20)$$

Using (18):

$$L = \frac{74.19}{2648400 I_{o \min}} = 3.70 \mu\text{H} \quad (21)$$

B. CAPACITOR

The capacitors used in capacitor bank is $2200 \mu\text{F} \times 25 \text{ V}$ with $R_{se} = 0.018 \Omega$ each, where A is the number of capacitors, therefore, $C = 2200 \times 10^{-6} \times A$ and $R_{se} = 0.018/A$. Using in (9):

$$0.72 \geq \frac{0.011}{A} + \frac{9.99}{A} + \frac{0.27}{A} + \frac{5.26}{A}$$

$$A \geq 22 \text{ capacitors} \quad (22)$$

C. TRANSFORMER

Used $B_{\max} = 0.2 \text{ T}$ considering losses hysteresis and not obtain overheated core transformer in (10) and (11).

$$B = \frac{V_{i \min}}{V_{i \max}} 2B_{\max} = 0.24 \text{ T} \quad (23)$$

$$N_1 \geq \frac{V_{i \min} D_{\max}}{A_e B f_{\text{conv}}} = 16 \text{ esp} \quad (24)$$

According the Fig. 1, using two transformers in parallel fold the transformation ratio, using (12).

$$N' = 2N = \frac{4D_{\max} (V_{i \min} - 2V_{SD})}{V_o + 2D_{\max} V_F} = 26.484 \quad (25)$$

According with new transformation ratio (N'): $N_2 = 1 \text{ turn}$ and $N_1 = 26 \text{ turn}$.

Using (13) and (14):

$$I_{sec_{RMS}} = I_o \sqrt{2D_{\max}} = 284.60 \text{ A} \quad (26)$$

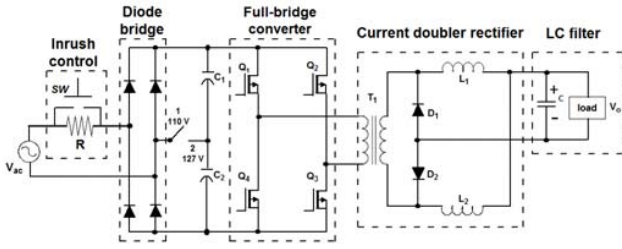


Fig. 12 Circuit topology of adopted converter with current doubler rectifier

$$A_{Cu_{sec}} = \frac{I_{sec_{RMS}}}{J} = 1.23 cm^2 \quad (27)$$

Using copper tape with 3.3 cm of width according (14), the depth is 3.7 mm.

$$I_{pri_{RMS}} = \frac{I_{sec_{RMS}}}{N'} = 10.75 A \quad (28)$$

$$A_{Cu_{sec}} = \frac{I_{pri_{RMS}}}{J} = 0.0466 cm^2 \quad (29)$$

The primary copper area is obtained in (29) and is equivalent eighteen wires AWG23.

VI. CIRCUIT CONFIGURATION

Fig. 12 shows the circuit topology of the adopted AC/DC converter. A diode bridge rectifier is used to convert the AC voltage to an uncontrolled DC voltage (V_{in}).

A full-bridge converter based on the phase-shift PWM (Pulse Width Modulation) technique is employed to generate a quasi-square wave voltage to transformer primary winding as shown in Fig. 8.

The current doubler rectifier converts V_2 to a DC voltage to be filtered by the LC filter providing the output voltage (V_o).

VII. MOUNTING PROCEDURE

The SMPS must work with very high currents (300 A) and power over 4320 W so the procedure for use of modules as shown in Fig. 1 allows the flexibility and decrease the power required for each component.

Each converter module containing MOSFETs with their snubbers were assembled with the heatsink (lower box), above this in a aligned way was set the rectifier module to decrease the length of the bonds decreasing heat losses and space saving as Fig. 13.

The converter's transformer was mounted on a core EE-65/33/26 and the secondary winding was calculated in one loop and due to the skin effect at 50 kHz had to be carried out with a copper tape with a width of 33 mm and 3.3 mm in height since the quantity of copper necessary to achieve the required current precluded their construction (418 AWG23 wire), were

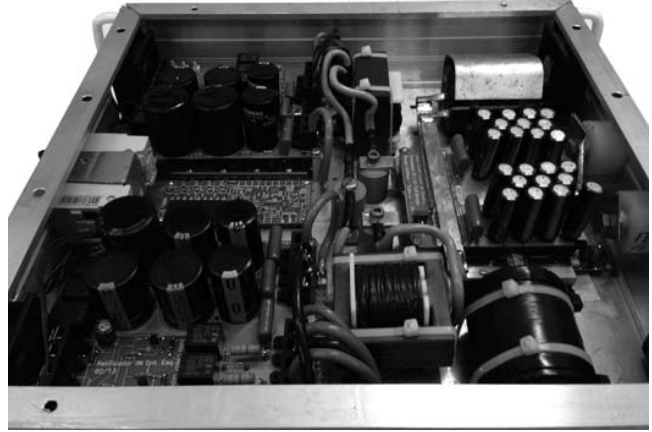


Fig. 13 Full source

placed between the winding copper tape grounded to the negative of the rectifiers to eliminate interference, shielding the transformer through the Faraday shield [20].

The inductors in the same way as the transformer due to the skin effect which occurs at 50 kHz should be constructed with 351 wires AWG25 so we used a copper tape of 3.3 mm width and 1.7 mm in height, winding up to reach the minimum required inductance of $3.70 \mu H$ [19], [20], [23].

The transformers and inductors were fixed orthogonally seeking noise reduction and decoupling of the magnetic components as shown in Fig. 13 [20].

The rectification and filtering module was divided into a rectifier module containing the schottky diodes and snubbers and a filter module which was superimposed containing the capacitor bank seeking to decrease the length of the links, the consequential losses due to the Joule effect and saving space as shown in Fig. 13 [20].

VIII. EXPERIMENTAL RESULTS

The experimental results for a 4.32 kW, 14.4 V/300 A rectifier with 127/220 V_{AC} and 50 kHz switching frequency are show in Fig. 14 and Fig. 15.

The waveform of a drive output control circuit of four isolated pulses at full load as shown in Fig. 14, where duty cycle means 0.45.

The primary voltage waveform at full load as show in Fig. 15. The characteristic of full-bridge with current doubler converter is clear in this figure.

The measured converter efficiency under full load is shown in Fig. 16 and the regulation is 0.42%.

IX. CONCLUSION

The full-bridge with current doubler converter proved efficient for use in high power corresponding to the proposed power project of 4320 W, the modular form used provided

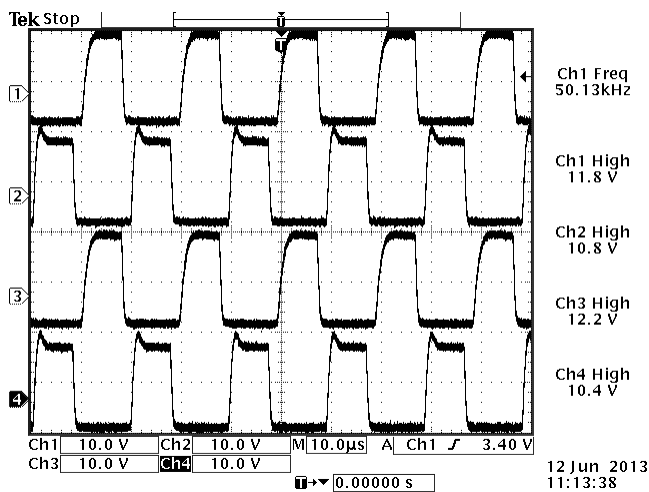


Fig. 14 Waveform of a drive output control circuit of four isolated pulses at full load

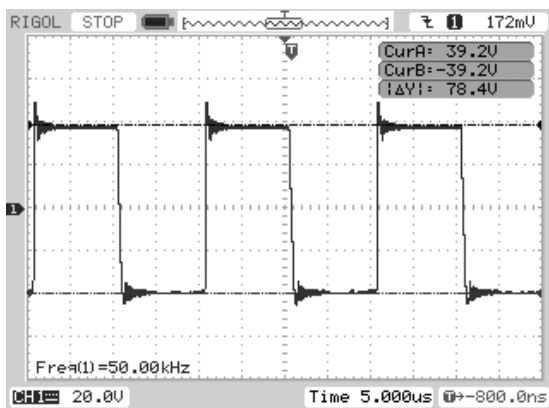


Fig. 15 Waveform of output transformers

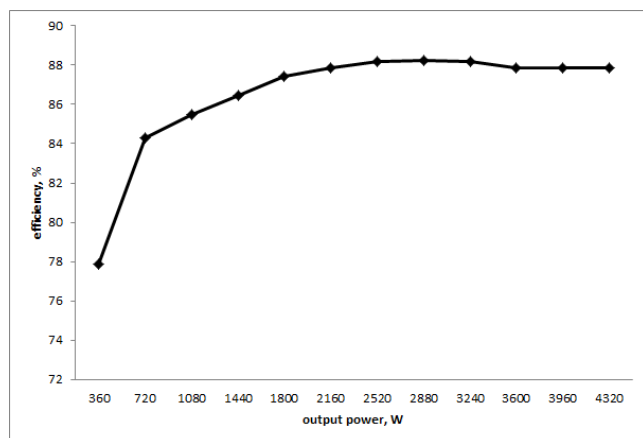


Fig. 16 Waveform of efficiency

the initially stipulated.

The implemented analog control circuit is quite compact due to the use of SMD components and may be used in any type of converter having several control features: thermal; inrush current; the output voltage (allowing closed-loop work) having the possibility of working as a current source and the emergency stop feature. Included are the drives required for any type of converter allowing their widespread use.

Several precautions were taken to control RFI, such as Faraday shielding in transformers, minimization of current loops in the power circuit, reducing the length of connections with the consequent reduction of harmonics, the decoupling of the magnetic components seeking orthogonal alignment between them.

The average efficiency of adopted converter is 86%, about 4.8% lower of a traditional converter as [18]. This is explained by the high power used.

The aim of the present paper was achieved because the end result was a robust source with high power density, galvanically isolated and with great commercial feasibility.

REFERENCES

- [1] *Manual de Baterias Bosch*, Bosch, 2007. [Online]. Available: <http://www.bosch.com.br/br/autopecas/produtos/baterias/downloads>
- [2] A. Bates, D.J. e Malvino, *Eletrônica* (v.1). MCGRAW HILL - ARTMED, 1997, no. v. 1.
- [3] I. Barbi, *Eletrônica de potência: projetos de fontes chaveadas*. Ed. do autor, 2007.
- [4] W. Cipelli, A.M.V. e Sadrini, *Teoria e desenvolvimento de projetos de circuitos eletrônicos*. São Paulo: Érica, 2004.
- [5] I. Barbi, *Eletrônica de potência*. Florianópolis: Ed. do Autor, 2006.
- [6] M. Rashid, *Eletrônica de potência: circuitos, dispositivos e aplicações*. São Paulo: Makron, 1999.
- [7] A. Ahmed, *Eletrônica de potência*. São Paulo: Pearson Education do Brasil, 2000.
- [8] R. Boylestad, *Dispositivos Eletrônicos e Teoria de Circuitos*. Rio de Janeiro: Ltc, 1999.
- [9] K. Sedra, A.S. e Smith, *Microeletrônica*. São Paulo: Pearson Makron Books, 2000.
- [10] R. W. Erickson and D. Maksimovic, *Fundamentals of power electronics*. Springer, 2001.
- [11] M. S. Ortmann, S. A. Mussa, and M. L. Heldwein, "Generalized analysis of a multistate switching cells-based single-phase multilevel pfc rectifier," *Power Electronics, IEEE Transactions on*, vol. 27, no. 1, pp. 46–56, 2012.
- [12] G. J. Schiavon, "No-break 1,2kva, senoidal, operando em malha fechada: Circuito de potência, circuito de controle analógico e circuito de controle digital com dsc," Master's thesis, Universidade Estadual de Londrina, 12 2007.
- [13] *SG3525A - Regulating Pulse Width Modulators*, STMicroelectronics, 2000. [Online]. Available: <http://www.st.com>
- [14] N. H. Kutkut, "A full bridge soft switched telecom power supply with a current doubler rectifier," in *Telecommunications Energy Conference, 1997. INTELEC 97., 19th International*. IEEE, 1997, pp. 344–351.
- [15] H. Chiu, L. Lin, Y. Su, and S. Mou, "A phase-shifted zero voltage transition full-bridge converter with current doubler synchronous rectification," in *SICE 2004 Annual Conference*, vol. 1. IEEE, 2004, pp. 60–65.
- [16] W.-J. Lee, C.-E. Kim, G.-W. Moon, and S.-K. Han, "A new phase-shifted full-bridge converter with voltage-doubler-type rectifier for high-efficiency pdp sustaining power module," *Industrial Electronics, IEEE Transactions on*, vol. 55, no. 6, pp. 2450–2458, 2008.

flexibility to the project allowing obtaining higher powers than

- [17] B.-Y. Chen and Y.-S. Lai, "Switching control technique of phase-shift-controlled full-bridge converter to improve efficiency under light-load and standby conditions without additional auxiliary components," *Power Electronics, IEEE Transactions on*, vol. 25, no. 4, pp. 1001–1012, 2010.
- [18] B.-R. Lin, K. Huang, and D. Wang, "Analysis and implementation of full-bridge converter with current doubler rectifier," in *Electric Power Applications, IEE Proceedings-*, vol. 152, no. 5. IET, 2005, pp. 1193–1202.
- [19] L. De Mello, *Projeto de Fontes Chaveadas - Teoria e Prática*. Érica, 2011.
- [20] C. H. Treviso, "Retificador de 6kw, fator de potência unitário, trifásico, comutação não dissipativa na conversão cc/cc e controle sincronizado em frequência," Ph.D. dissertation, Universidade Federal de Uberlândia, 1999.
- [21] A. L. B. Ferreira, "Ups de 5kv a, tipo passive stand-by, com integração de painéis solares," Master's thesis, Universidade Estadual de Londrina, 8 2009.
- [22] C. McLyman, *Transformer and inductor design handbook*, ser. Transformer and Inductor Design Handbook. New York: M. Dekker, 1978, no. v. 7.
- [23] R. L. Alves, "Fontes auxiliares de alimentação para conversores de alta potência e elevada tensão no barramento cc," Master's thesis, Universidade Federal de Santa Catarina, 2 2003.



Júlio Cesar Lopes de Oliveira received the B.S. degree in electrical engineering from the Federal University of Paraná (UFPr), Curitiba, Brazil, in 1991.

He is currently an adjunct Professor with the Pitagoras University, Londrina, Brazil and currently working toward M.S. degree with the Department of Electrical Engineering of Londrina State University (UEL), Londrina, Brazil.

His research interests include modeling, design and control of power converters, soft-switching

techniques, electric drive systems, dc-dc converters.



Carlos Henrique Gonçalves Treviso completed his bachelor's degree in Electrical Engineering in 1992, became Master in 1994 and PhD in Electrical Engineering in 1999 from the Federal University of Uberlândia. Was coordinator of the Electrical Engineering between 2000 and 2001. He served as deputy director of the Center for Technology and Planning (2002-2006), State University of Londrina (UEL). Between 2008 and 2011 he was head of the department of Electrical Engineering (UEL). Also advises businesses. His research includes: power

electronics, power quality and energy efficiency, electronic control systems and electric drive machines. Currently doing a postdoctoral fellow at the Federal University of Santa Catarina, Brazil.